# IDENTIFICATION OF PARTLY DESTROYED OBJECTS USING DEFORMABLE TEMPLATES

HÅVARD RUE* AND ODDVAR K. HUSBY

DEPARTMENT OF MATHEMATICAL SCIENCES

NTNU, NORWAY

MARCH 1997

ABSTRACT

This article addresses the problem of identification of partly destroyed human melanoma cancer cells in confocal microscopy imaging. Complete cancer cells are nearly circular and most of them have a nearly homogeneous boundary and interior region. A *deformable template* (Grenander, 1993) is well suited for these complete cells and models a cell as a natural deformed template or prototype. We will in this article focus on the remaining cells which have lost parts of the boundary region most probably due to a "capping" phenomenon. We can interpret these cells as being partly destroyed, where in our statistical model the lost part of the boundary region is generated by a *destructive deformation field* acting and living *on* the cell or template. By doing simultaneous inference for both the natural and destructive deformation field, we are able to obtain reliable estimates of the outline in addition to where on the boundary the cell is destroyed. We apply our model to identifying partly destroyed human melanoma cancer cells with good results.

KEYWORDS: Deformable Templates; Destructive deformations; Markov chain Monte Carlo methods; Object identification; Object recognition.

*ADDRESS FOR CORRESPONDENCE: Department of Mathematical Sciences, Norwegian University of Science and Technology, N-7034 Trondheim, Norway.

E-MAIL: Havard.Rue@math.ntnu.no

# 1 INTRODUCTION

High level statistical imaging is an area of increasing research interest, but it is still at an early stage. The results from the last few years of research within low-level image analysis and stochastic simulation methods have prepared the way for more high-level models within imaging. The goal for high-level models is *understanding* rather than *processing* of images, for example in tasks such as counting the number of cells in a confocal microscopy image and classifying them into different types, and giving reliable uncertainty estimates for global properties of objects in a scene. Such questions and applications demand high-level interpretation, which in turn requires high-level models and inference. A theoretical framework for representing knowledge in complex systems (*pattern theory*) was developed by U. Grenander through the 70's and 80's. The theory is now collected in a monograph (Grenander, 1993) while limited applications to date are surveyed and discussed in Grenander and Miller (1994). High-level models can in this framework be constructed from various deformation mechanisms action on prototypes, the *deformable template* approach. It is commonly accepted that the deformable template and also the stochastic geometry approach (Baddeley and van Lieshout, 1993), have a promising potential for modeling and structuring information in high-level imaging problems. Work by Rue and Hurn (1997) combines both of the approaches in an object recognition application. Refer also to Grenander and Miller (1994) and Jain, Zhong and Lakshmanan (1996) for a list of references.

This work is motivated from an application of object recognition in confocal microscopy imaging studying human melanoma cancer cells, where the goal was to estimate the number of cells and the outline of each cell in the image (as the input for further processing and study). Most of the cells are nearly circular with a near homogeneous boundary and interior region, for which a deformable template is well suited as a model for the outline. (The template model can be embedded into a marked point process framework to handle the case of a random number of objects. We will not elaborate in these directions here, but refer the reader to Baddeley and van Lieshout (1993), Rue and Syversveen (1997), Rue and Hurn (1997) and Qian and Mardia (1995) for further details and applications.) We will in this article focus on the remaining cells that have lost parts of the boundary region, most probably due to a *capping* phenomena; some of the antibodies (producing the contrast) tend to cluster on the surface membrane, leaving parts of the surface with fewer antibodies (and less contrast). Three such cells appear in Figure 11. Unless we take into account that parts of the boundary can be lost, the estimated outline of the cell will have severe bias (as shown in Section 5). We can however interpret these cells as being partly destroyed regular cells, where the lost part of the boundary is caused by a *destructive deformation field* acting and living *on* the cell or template in our statistical model. This approach was suggested by Grenander (1993, Remark 16.2.3). Our contribution in this article is to demonstrate that a destructive deformation field is well suited to model partly destroyed cells or objects, and makes it possible to estimate simultaneously the outline and which parts of the cell boundary are destroyed.

The outline of the article is as follows: In Section 2, we will give a brief introduction to the deformable template approach of Grenander (1993) appropriate for modeling nearly circular cells. In Section 3, we introduce a destructive deformation field to model partly destroyed objects like those in Figure 1. We discuss inference from the model in Section 4, and show in Section 5 the results of applying our model to the partly destroyed human melanoma cancer cells in Figure 1.

## 2 A DEFORMABLE TEMPLATE MODEL

This section introduces a deformable template model for the outline of an object following Grenander, Chow and Keenan (1991), and discusses how we can use the model to identify cells similar to those in Figure 1, but without a destroyed boundary region.

### 2.1 THE BASIC MODEL

We use as the template or ideal prototype for a cell, a closed polygon in $\Re^2$ with $n$ vertices, and with shape similar to a circle. Figure 22 shows the polygon template with $n = 8$ line-segments $g_0, g_1, \ldots, g_{n-1}$. To allow for natural variation of the cell, each $g_i$ is allowed to deform. We write a deformed line-segment as $s_i g_i$, where

$$s_i = \begin{bmatrix} 1 + t_{0i} & t_{1i} \\ -t_{1i} & 1 + t_{0i} \end{bmatrix}$$

is a scale-rotation matrix with stochastic elements $t_{0i}$ and $t_{1i}$. We let $\boldsymbol{t}_0 = (t_{0i})$ and $\boldsymbol{t}_1 = (t_{1i})$ be independent and identical Gaussian distributed with zero mean and covariance matrix $\boldsymbol{\Sigma}$. We follow Grenander et al. (1991) and let the density for $t_{0i}$ conditional on the rest of $\boldsymbol{t}_0$, only depend on $t_{0,i-1}$ and $t_{0,i+1}$ (where indices are modulus $n$), i.e. $\boldsymbol{t}_0$ is a first order cyclic Gaussian Markov random field. The only non-zero terms in $\boldsymbol{\Sigma}^{-1}$ are then $\Sigma^{ii}$ and $\Sigma^{i,j+1}$, where $\Sigma^{ij}$ is the $ij$-th element in $\boldsymbol{\Sigma}^{-1}$. We write these elements as

$$\Sigma^{ii} = a_0/n + 2a_1 n^2, \quad \text{and} \quad \Sigma^{i,j+1} = \Sigma^{i,j-1} = -a_1 n^2. \tag{1}$$

The parameterization in (1) ensures that the behavior is not too dependent on $n$ (as shown by a limit argument by Kent, Mardia and Walder (1996)). The parameters $a_0$ and $a_1$ have nice interpretations using standard results for normal variables; $1/\Sigma^{ii}$ controls the variability around the template, and

$-\Sigma^{i,j+1}/\Sigma^{ii}$ controls the smoothness of deviation from the template (Kent et al., 1996). As the template is a closed polygon, we need to constrain the deformations $s_i$ to satisfy the *linear* closure constraint $\sum_i s_i g_i = 0$. This constraint makes $\boldsymbol{t}_0$ and $\boldsymbol{t}_1$ dependent but the joint density is still Gaussian. Denote by $\pi(\boldsymbol{t}_0, \boldsymbol{t}_1)$ and $\pi^*(\boldsymbol{t}_0, \boldsymbol{t}_1)$ the corresponding joint unconditional and conditional Gaussian density for $\boldsymbol{t}_0$ and $\boldsymbol{t}_1$. (In Section 4 we will show that there is no need to compute the conditional density $\pi^*(\boldsymbol{t}_0, \boldsymbol{t}_1)$.)

To use the deformable template model to locate a single cell in the image $\boldsymbol{y} = \{y_i, i \in \mathcal{S}\}$, we need to specify a position $c$ to place the template in the image, and also a likelihood model $L(\boldsymbol{y};\ \boldsymbol{t}_0, \boldsymbol{t}_1, c)$ connecting the parametric template model with the data $\boldsymbol{y}$. Figure 33 illustrate the likelihood model we will use. The function $R(i;\ \boldsymbol{t}_0, \boldsymbol{t}_1, c)$ provides the required link, labelling each pixel $i$ in the image as one of three classes, background (white, $R = 0$), boundary (black, $R = 1$) and interior (grey, $R = 2$), based on the outline of the deformed template. We assume further that $y_i$ is Gaussian with mean $\mu_R$ and variance $\sigma_R^2$, where $R = R(i;\ \boldsymbol{t}_0, \boldsymbol{t}_1, c)$ indicates the class to which pixel $i$ belongs (see Figure 3). The posterior density for the unknown parameters is then

$$\pi^*(\boldsymbol{t}_0, \boldsymbol{t}_1, c \mid \boldsymbol{y}) \propto \frac{1}{|\mathcal{S}|}\ \pi^*(\boldsymbol{t}_0, \boldsymbol{t}_1)\ \exp\left(-\frac{1}{2}\sum_{i \in \mathcal{S}}\left(\frac{y_i - \mu_{R(i;\,\boldsymbol{t}_0,\boldsymbol{t}_1,c)}}{\sigma_{R(i;\boldsymbol{t}_0,\boldsymbol{t}_1,c)}}\right)^2\right), \tag{2}$$

assuming independence for the $y_i$'s and an uniform prior for the position $c$. For later usage, define $\pi(\boldsymbol{t}_0, \boldsymbol{t}_1, c \mid \boldsymbol{y})$ to be the posterior density with $\pi(\boldsymbol{t}_0, \boldsymbol{t}_1)$ instead of $\pi^*(\boldsymbol{t}_0, \boldsymbol{t}_1)$ in (2).

All inference concerning the parameters in the model is now based on the posterior density (2). The posterior density is analytically intractable so we need to rely on Markov chain Monte Carlo (MCMC) methods to investigate its properties. We will postpone this topic until Section 4, and instead study how we can modify the model to handle partly destroyed cells like those in Figure 1.

# 3 Modeling Partly Destroyed Objects

The model presented in Section 2 is not suitable to model the cells in Figure 1 where parts of the boundary regions are lost. The likelihood term needs information about where on the boundary region the cell is destroyed. We will introduce a destructive deformation field living *on* the template, as the required tool to model partly destroyed objects.

To model the destructive deformation field, we introduce a binary field $\boldsymbol{x} = (x_i)$ with dimension $n$. The field $\boldsymbol{x}$ lives *on* the template as illustrated in Figure 45. We define the boundary region along the line-segment $s_i g_i$ to be destroyed if $x_i = 1$, and not destroyed if $x_i = 0$. (In some applications it will be more reasonable to increase the dimension of $\boldsymbol{x}$, and allow for two or more $x_i$'s on each or some of the $g_i$'s.) A natural first choice for the density for $\boldsymbol{x}$, is a first order cyclic Markov random field,

$$\pi(\boldsymbol{x}) \propto \exp\left(\beta_0 \sum_i 1_{[x_i=1]} + \beta_1 \sum_i 1_{[x_i=x_{i+1}]}\right), \tag{3}$$

where addition is modulo $n$. The parameter $\beta_0$ controls how much of the boundary region is destroyed, and $\beta_1$ controls the continuity of $\boldsymbol{x}$. We can estimate $\beta_0$ and $\beta_1$ using the observation that most of the partly destroyed cells have lost around $30 - 40\%$ of boundary region and the lost part is a single connected piece. Thus we take Pr$(x_i = 1) \approx 1/3$ and Pr$(x_i = x_{i+1}) \approx 1 - 2/n$. We estimated these probabilities (as a function of $\beta_0$, $\beta_1$ and $n$) using simulations from (3), and then we simply inverted the table to obtain the corresponding values for $\beta_0$ and $\beta_1$. (We could improve the estimates using the empirical average of these properties instead of using the modal value. The final result is not too dependent of $\beta_0$ and $\beta_1$ for reasonable values.)

The likelihood function needs to be informed where on the template the data are to be considered as destroyed when we use the destructive deformation field. Figure 54 shows this situation. The destroyed parts of the deformable templates map to a new third class with the label *destroyed* (light grey, $R = 3$). The density for the data in the destroyed region will depend on the application. For our data in Figure 1, the destroyed boundary region appears as an interior region ($R = 2$) meaning that $y_i$ is Gaussian with parameters $\mu_3 = \mu_2$ and $\sigma_3^2 = \sigma_2^2$. If the data in the destroyed region are badly corrupted, then the choice $\sigma_3^2 = \infty$ and $\mu_3 = 0$ might be appropriate. We take $\boldsymbol{x}$ and $(\boldsymbol{t}_0, \boldsymbol{t}_1)$ to be a-priori independent so the posterior density becomes

$$\pi^*(\boldsymbol{x}, \boldsymbol{t}_0, \boldsymbol{t}_1, c \mid \boldsymbol{y}) \propto \frac{1}{|\mathcal{S}|}\, \pi(\boldsymbol{x})\ \pi^*(\boldsymbol{t}_0, \boldsymbol{t}_1)\ \exp\left(-\frac{1}{2}\sum_{i\in\mathcal{S}}\left(\frac{y_i - \mu_{R(i;\,\boldsymbol{x},\boldsymbol{t}_0,\boldsymbol{t}_1,c)}}{\sigma_{R(i;\,\boldsymbol{x},\boldsymbol{t}_0,\boldsymbol{t}_1,c)}}\right)^2\right). \tag{4}$$

We are now able to estimate jointly the position, the deformation of the template and the destructive deformation field from partly destroyed cells or objects using (4). (Note that (4) can be used for other templates or prototypes also, as only the constant vectors $g_i$ changes.) Again, the posterior density is analytically intractable but Markov chain Monte Carlo methods can be used to explore the density. This is the topic for the following section.

## 4 INFERENCE

The posterior density for deformable template model with or without the destructive deformation field (Eq. (2) and Eq. (4)), can be explored using Markov chain Monte Carlo (MCMC) methods. There is now a rich literature on MCMC methods, and Gilks, Richardson and Spiegelhalter (1996) provides a comprehensive overview of theory and applications.

The basic idea in MCMC is as follows. To generate realizations from $f(dz)$, say, we construct an irreducible and aperiodic transition kernel to obtain a reversible Markov chain with $f(dz)$ as the equilibrium distribution. The Markov chain will give dependent samples from the target distribution after convergence. We will only make use of the *Metropolis* algorithm, which goes as follows. Let $z$ be the current state of the Markov chain. We propose a move of type $j$ that moves $z$ to $dz'$ with probability $q_j(z, dz')$, satisfying $q_j(z, dz') = q_j(z', dz)$. This move is accepted with probability $\alpha_j(z \to z') = \min(1, f(dz')/f(dz))$, otherwise we remain in the old state $z$.

To generate samples from the posterior density (4) (or (2) after obvious changes), we will make use of the following three basic move types.

1. Propose a new position $c' = c + u_c$ for the template, where $u_c$ is a random point in a disc centred at the origin with radius $r_c$ (keeping the remaining parameters fixed). This move-type is most useful in the early stages to help locate the object.

2. Let $v_i$ be the vertices of the deformable template. Select one of the $n$ vertices at random, $i$ say, and propose to change $v_i$ to $v_i' = v_i + u_v$ where $u_v$ is a random point in a disc centered at the origin with radius $r_v$ (keeping the remaining parameters fixed).

3. Select one of the $x_i$'s at random, and propose to change the value of $x_i$ to $x_i' = 1 - x_i$ (keeping the remaining parameters fixed).

The proposed new state is then accepted with probability

$$\begin{aligned} \alpha_j((\boldsymbol{x}, \boldsymbol{t}_0, \boldsymbol{t}_1, c) \to (\boldsymbol{x}, \boldsymbol{t}_0, \boldsymbol{t}_1, c)') &= \min\left(1, \frac{\pi^*((\boldsymbol{x}, \boldsymbol{t}_0, \boldsymbol{t}_1, c)' \mid \boldsymbol{y})}{\pi^*(\boldsymbol{x}, \boldsymbol{t}_0, \boldsymbol{t}_1, c \mid \boldsymbol{y})}\right) \\ &= \min\left(1, \frac{\pi((\boldsymbol{x}, \boldsymbol{t}_0, \boldsymbol{t}_1, c)' \mid \boldsymbol{y})}{\pi(\boldsymbol{x}, \boldsymbol{t}_0, \boldsymbol{t}_1, c \mid \boldsymbol{y})}\right), \end{aligned} \tag{5}$$

where we make use of the identity $\pi(\boldsymbol{w}')/\pi(\boldsymbol{w}) = \pi(\boldsymbol{w}'|\boldsymbol{A}\boldsymbol{w}' = \boldsymbol{b})/\pi(\boldsymbol{w}|\boldsymbol{A}\boldsymbol{w} = \boldsymbol{b})$ for any vector $\boldsymbol{w}$ and $\boldsymbol{w}'$ (see Appendix). Note also that there is no need to compute the conditional density $\pi^*(\boldsymbol{t}_0, \boldsymbol{t}_1)$ as the unconditional density will do. Note that (5) reduces to simple expressions for each of the three move types. (For example in move-type 1, (5) is the likelihood ratio of the new and old state.) This is because only a few of the variables are updated in each step, which causes terms in the posterior density to cancel.

If we want to avoid self-intersecting objects (i.e. restrict the polygons to be simple), we simply reject all proposals that self-intersect and accept the others using (5). The formal argument is to condition $(\boldsymbol{t}_0, \boldsymbol{t}_1)$ on the appropriate event obtaining $\pi^{**}(\boldsymbol{t}_0, \boldsymbol{t}_1)$, and then using the fact that $\pi^{**\prime}/\pi^{**}$ equals $\pi^{*\prime}/\pi^*$ which again equals $\pi'/\pi$ (for two configurations $(\boldsymbol{t}_0, \boldsymbol{t}_1)'$ and $(\boldsymbol{t}_0, \boldsymbol{t}_1)$).

We can use the output from the Markov chain to obtain point estimates for the outline of the object. The Bayesian procedure is to define a *loss* function $L((\boldsymbol{s}, c, \boldsymbol{x}), (\hat{\boldsymbol{s}}, \hat{c}, \hat{\boldsymbol{x}}))$ that specifies the loss or cost if we estimate the configuration as $(\hat{\boldsymbol{s}}, \hat{c}, \hat{\boldsymbol{x}})$ when it is really $(\boldsymbol{s}, c, \boldsymbol{x})$. The optimal Bayesian estimator (OBE), $(\hat{\boldsymbol{s}}, \hat{c}, \hat{\boldsymbol{x}})^*$, is the configuration which minimizes the posterior expectation of the loss (Bayes risk)

$$(\hat{\boldsymbol{s}}, \hat{c}, \hat{\boldsymbol{x}})^* = \arg \min_{(\hat{\boldsymbol{s}}, \hat{c}, \hat{\boldsymbol{x}})} \mathrm{E}\, L((\boldsymbol{s}, c, \boldsymbol{x}), (\hat{\boldsymbol{s}}, \hat{c}, \hat{\boldsymbol{x}})).$$

The most common choice is the zero-one loss, which lead to the maximum posterior mode (MAP) as the OBE. This choice is natural if the posterior density is unimodal, as is often the case with good data. The MAP estimate can be approximated by means of a simulated annealing algorithm (Geman and Geman, 1984). More complex and visually pleasing loss functions based on Baddeley (1992) *delta metric* are discussed by Rue and Syversveen (1997) and Rue and Hurn (1997), and these give better visual results most noticeable for moderate quality data. The computation of the OBE is then slightly more involved and makes use of the two-step algorithm of Rue (1995). In the examples in Section 5, we will use the MAP estimator, since the data in Figure 1 are good. To give a visual impression of the uncertainty involved, we also show some samples from the posterior density.

# 5 EXAMPLES

We will now present the results of applying an deformable template model, with and without the destructive deformation field, on the three partly destroyed cells shown in Figure 1.

We selected the parameters $a_0$ and $a_1$ (in Eq. (1)) by trial and error to obtain reasonable visual behavior when generating realizations from the prior density. This resulted in the values $a_0 = 400$ and $a_1 = 0.4$ using $n = 14$ line-segments. The parameters $\beta_0$ and $\beta_1$ in (3) was selected to match $\Pr(x_i = 1) = 1/3$ and $\Pr(x_i = x_{i+1}) = 1 - 2/n$, a choice giving reasonable results in most cases. The mean levels and variances of each class ($\mu_k$ and $\sigma_k^2$) were estimated from other similar images (but could also be treated as unknown parameters, see Rue and Syversveen (1997) and Hurn (1996)). The presented results are not heavily dependent on the selected parameters provided these are in a reasonable range.

Figure 66 and 77 both demonstrate typical behavior using the deformable template model without (image (a)) and with (image (b)) the destructive deformation field. The MAP estimates in Figure 6a and Figure 7a are indeed natural in the destroyed parts of the boundary region; to minimize the model error, the deformable template tries to minimize the length of the outline in that region. The destructive deformation field is able to detect where the boundary is destroyed (shown as thin lines in Figure 6b and Figure 7b), and the outline is well estimated. Figure 6c and Figure 6d (and similarly with Figure 7) show some nearly independent samples from the posterior densities to give a visual impression of the uncertainty involved. Figure 6d and Figure 7d show increased uncertainty in the destroyed region using the destructive deformation field, we would be expected.

To investigate the property of our model for low informative data we added additional independent Gaussian noise with zero mean and variance $100^2$ to Figure 1b as shown in Figure 88. The interpretation of Figure 8 is similar to Figure 6 and 7. The results are of course not so good as for Figure 6 and 7, but still Figure 8d is preferable to Figure 8c.

We have performed many experiments with various objects (other than circles), including cases when the data is missing in parts of the object. The experiments displayed here are typical. In our experience, a destructive deformation field is well able to model partly destroyed objects.

## ACKNOWLEDGMENT

Thanks to Mari Hjelstuen of the Biophysics group at NTNU, for providing the confocal microscopy data.

## A PROOF OF THE IDENTITY

Let $\boldsymbol{w} = (w_1, \ldots, w_n)$ be a random vector with density $\pi(\boldsymbol{w})$ and $\boldsymbol{A}$ be a $k \times n$-matrix with rank $k$. The identity $\pi(\boldsymbol{w}' | \boldsymbol{A}\boldsymbol{w}' = \boldsymbol{b}) / \pi(\boldsymbol{w} | \boldsymbol{A}\boldsymbol{w} = \boldsymbol{b}) = \pi(\boldsymbol{w}')/\pi(\boldsymbol{w})$ follows from the transformation $v_i = w_i$, $i = 1, \ldots, n-k$, and $v_{n-k+i} = (\boldsymbol{A}\boldsymbol{w})_i$, $i = 1, \ldots, k$, giving $\pi(\boldsymbol{v}) \propto \pi(\boldsymbol{w})$, and so $\pi(v_1, \ldots, v_{n-k} \mid v_{n-k+1}, \ldots, v_n) \propto \pi(\boldsymbol{v})$.

## REFERENCES

BADDELEY, A. J. (1992). Errors in binary images and a $L^p$ version of the Hausdorff metric, *Nieuw Archief voor Wiskunde* 10: 157–183.

BADDELEY, A. J. AND VAN LIESHOUT, M. N. M. (1993). Stochastic geometry models in high–level vision, *in* K. V. Mardia and G. K. Kanji (eds), *Statistics and Image*, Vol. 20, Abingdon: Carfax Publishing Co, chapter 11, pp. 235–256. Special issue Journal of Applied Statistics.

GEMAN, S. AND GEMAN, D. (1984). Stochastic relaxation, Gibbs distributions, and the Bayesian restoration of images, *IEEE Transactions on Pattern Analysis and Machine Intelligence* 6: 721–741.

GILKS, W. R., RICHARDSON, S. AND SPIEGELHALTER, D. J. (1996). *Markov Chain Monte Carlo in Practice*, Chapman & Hall.

GRENANDER, U. (1993). *General Pattern Theory*, Oxford University Press.

GRENANDER, U. AND MILLER, M. I. (1994). Representations of knowledge in complex systems (with discussion), *Journal of the Royal Statistical Society, Series B* 56(4): 549–603.

GRENANDER, U., CHOW, Y. AND KEENAN, D. M. (1991). *Hands: a Pattern Theoretic Study of Biological Shapes*, Research Notes on Neural Computing, Springer, Berlin.

HURN, M. A. (1996). Bayesian image analysis in confocal fluorescence microscopy, *Statistical Research Report 96:01*, School of Mathematical Sciences, Univeristy of Bath.

JAIN, A. K., ZHONG, Y. AND LAKSHMANAN, S. (1996). Object matching using deformable templates, *IEEE Transactions on Pattern Analysis and Machine Intelligence* 18(3): xxx–xxx.

KENT, J. T., MARDIA, K. V. AND WALDER, A. N. (1996). Conditional cyclic markov random fields, *Advances in Applied Probability (SGSA)* 28: 1–12.

QIAN, W. AND MARDIA, K. V. (1995). Recognition of multiple objects with occlusions, *Stat 95/01*, University of Leeds.

RUE, H. (1995). New loss functions in Bayesian imaging, *Journal of the American Statistical Association* 90: 900–908.

RUE, H. AND HURN, M. A. (1997). Bayesian object identification, *Statistics*, Department of Mathematical Sciences, Norwegian University of Science and Technology, Trondheim, Norway.

RUE, H. AND SYVERSVEEN, A. R. (1997). Bayesian object recognition with Baddeley's delta loss, *Advances in Applied Probability (SGSA)* XX: xx–xx.

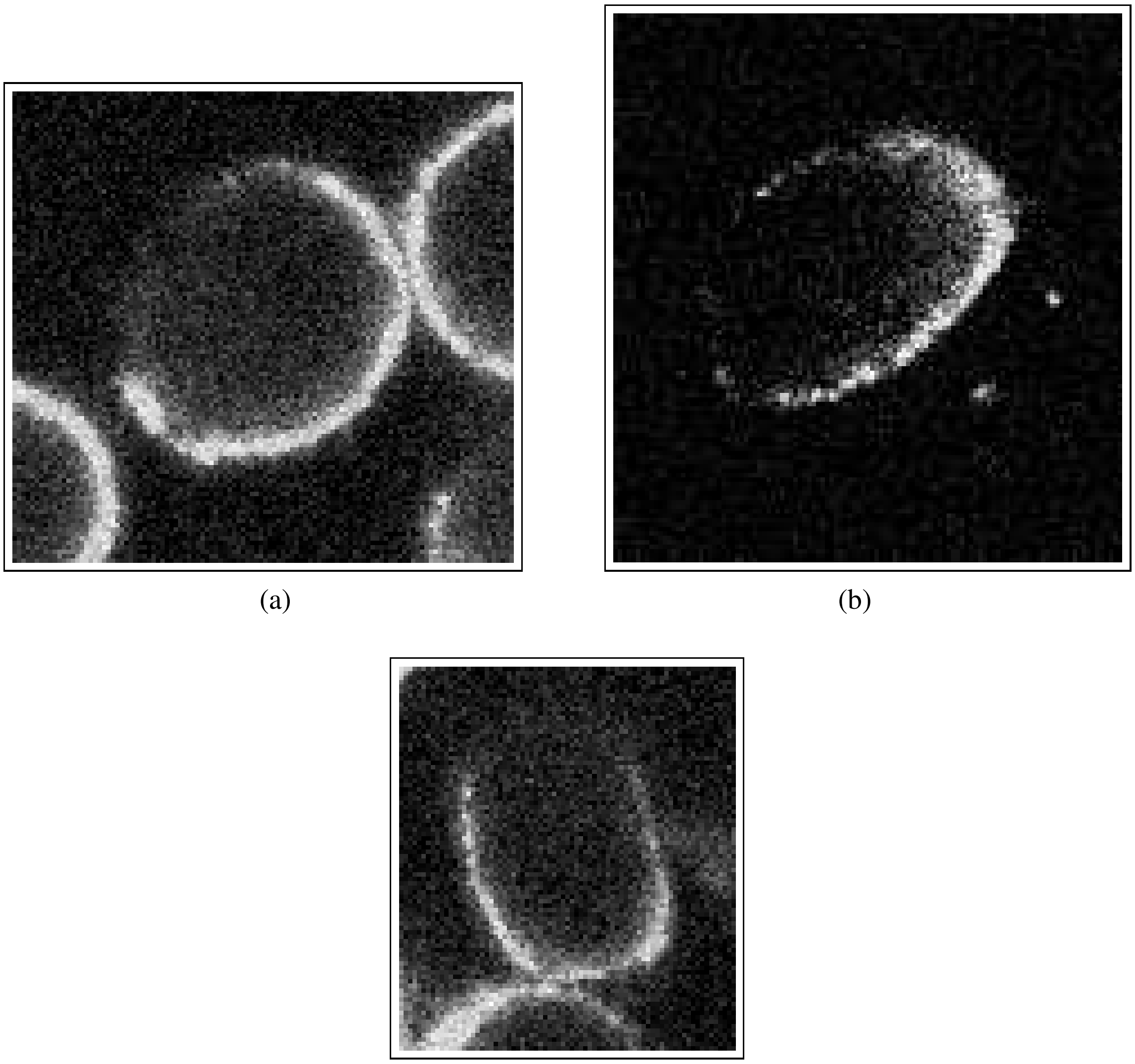

(a) (b)

(c)

FIGURE 1: Three confocal microscopy images of cells where parts of the boundary region is lost, most probably due to a “capping” phenomena as described in Section 1.

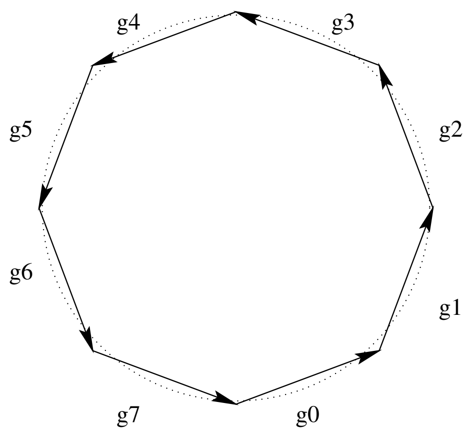


FIGURE 2: A circular polygon template with eight line-segments representing the dotted circle.

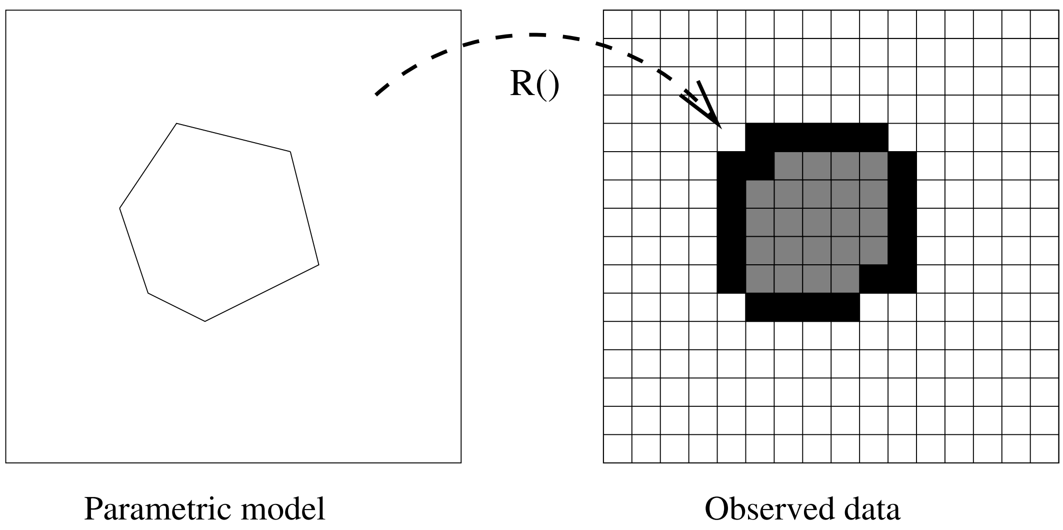


FIGURE 3: The link between the parametric world and the discrete observed data via the $R()$ function. The $R()$ function uses the deformed template to map the image into a *background* region (white), a *boundary region* (black) and an *interior region* (grey).

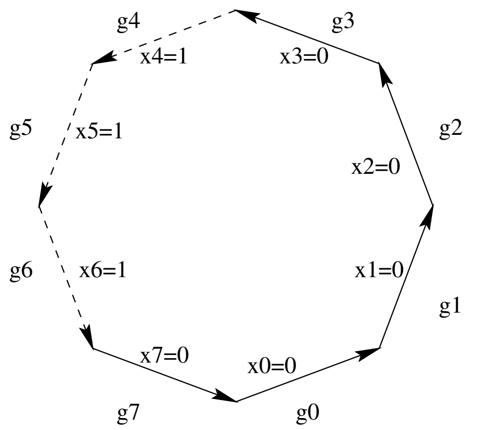


FIGURE 4: An example of a circular polygon template with a binary destructive deformation field, where boundary region along the dashed lines are destroyed.

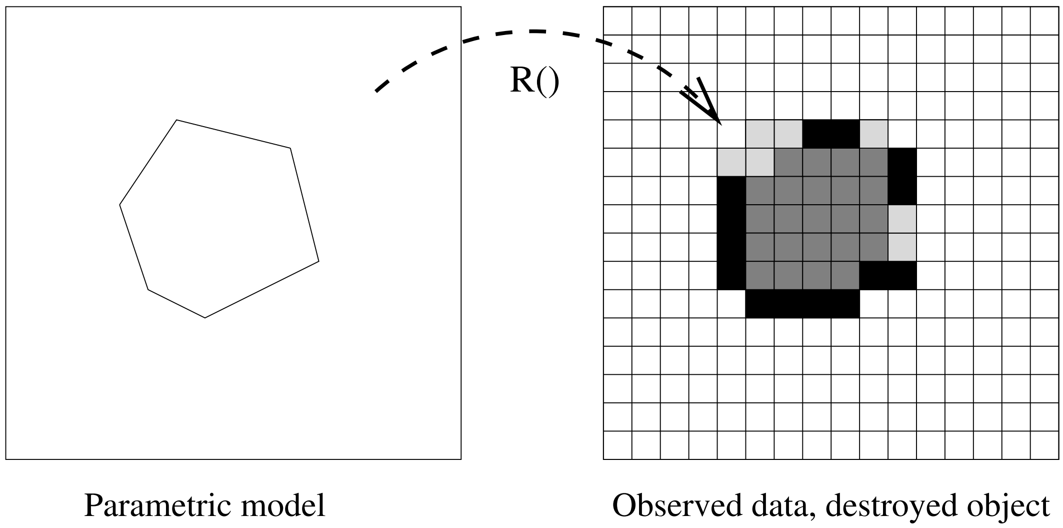


FIGURE 5: The link between the parametric world and the discrete observed data when destructive deformation field is used. The $R()$ function segments the image into a *background* region (white), a *boundary region* (black), a *destroyed boundary region* (light grey) and an *interior region* (grey).

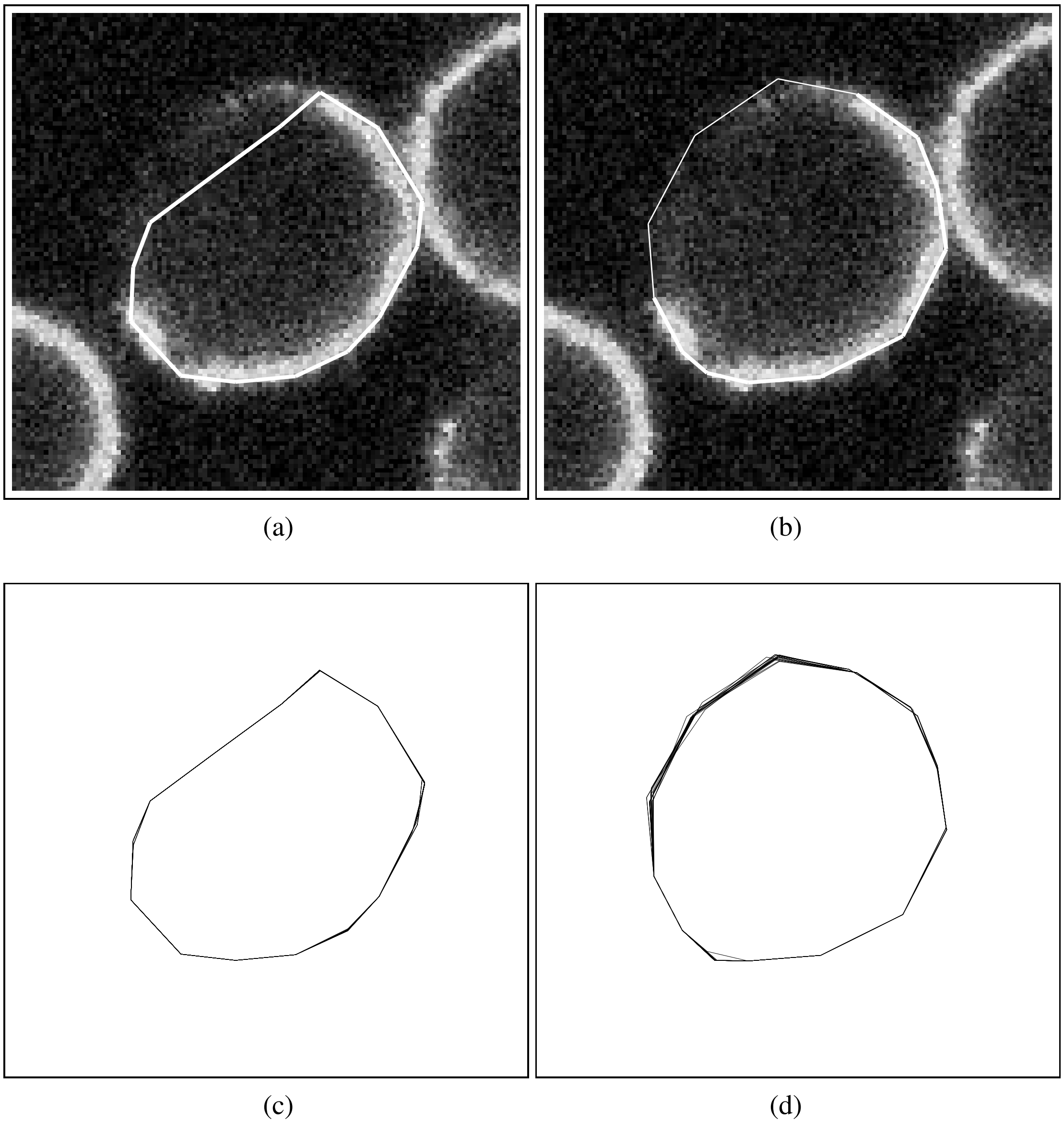

FIGURE 6: The results of applying the various models to the data in Figure 1a: (a) the MAP estimate using a deformable template model; (b) the MAP estimate using a deformable template model together with a destructive deformation process; (c) samples from the posterior density giving visual uncertainty estimates for (a); (d) samples from the posterior density giving visual uncertainty estimates for (b).

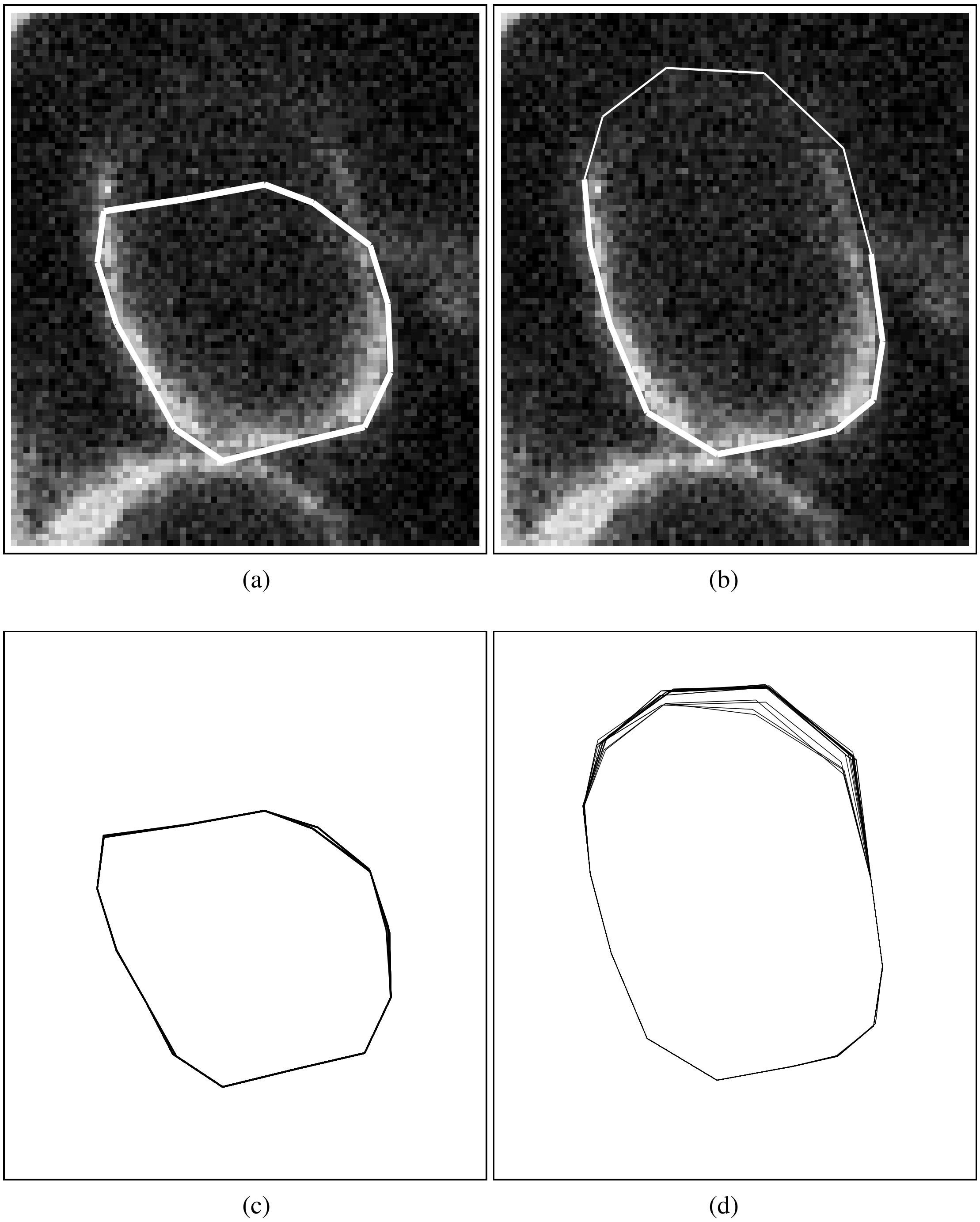


FIGURE 7: The results of applying the various models to the data in Figure 1c: (a) the MAP estimate using a deformable template model; (b) the MAP estimate using a deformable template model together with a destructive deformation process; (c) samples from the posterior density giving visual uncertainty estimates for (a); (d) samples from the posterior density giving visual uncertainty estimates for (b).

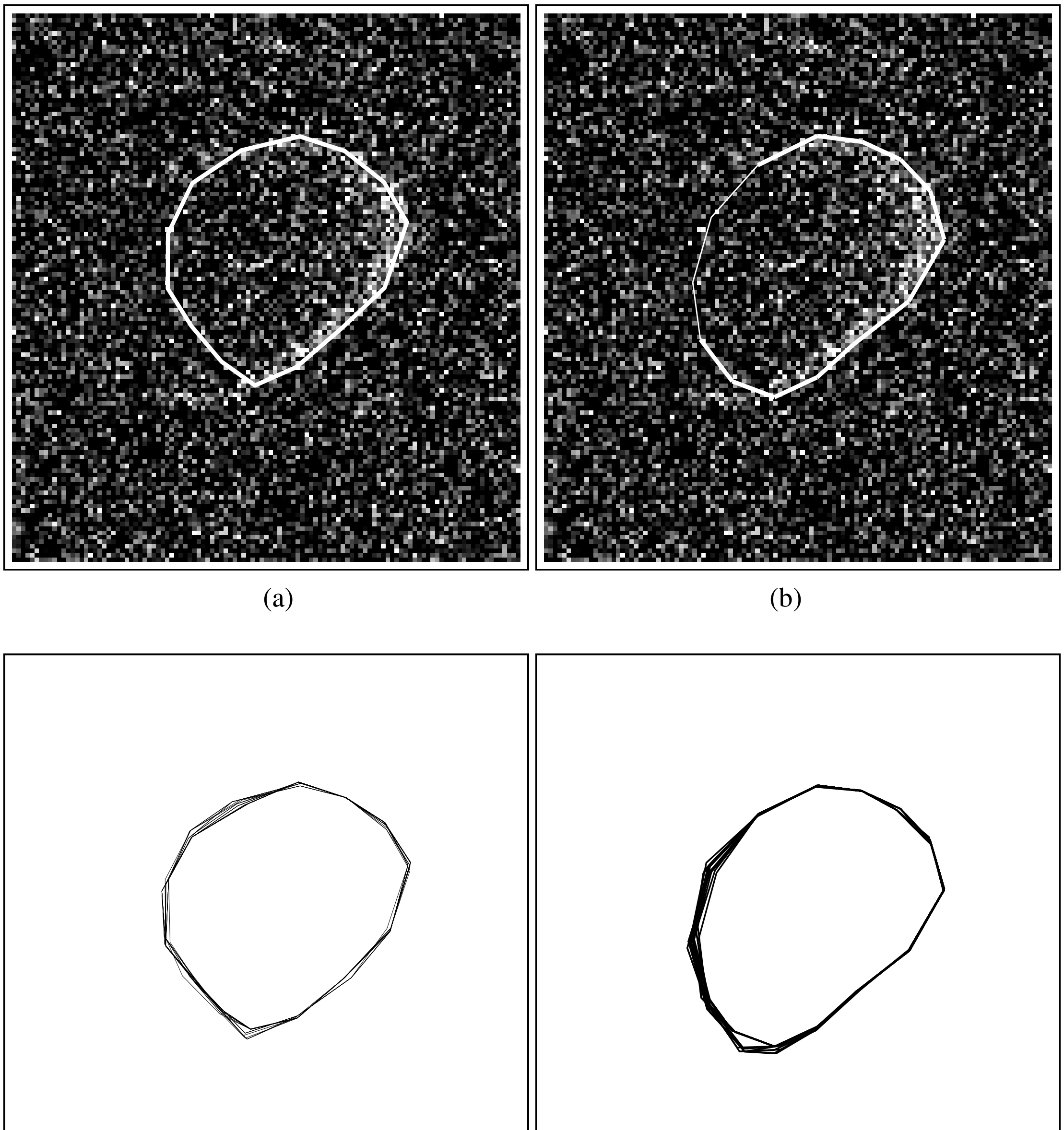

(a) (b)

(c) (d)

FIGURE 8: The results of applying the various models to the data in Figure 1b with additional independent Gaussian noise added to each pixel: (a) the MAP estimate using a deformable template model; (b) the MAP estimate using a deformable template model together with a destructive deformation process; (c) samples from the posterior density giving visual uncertainty estimates for (a); (d) samples from the posterior density giving visual uncertainty estimates for (b).